Multifront regime of a piecewise-linear FitzHugh-Nagumo model with cross diffusion

Evgeny P. Zemskov,[1,*] Mikhail A. Tsyganov,[2,†] and Werner Horsthemke[3,‡]

[1]*Federal Research Center for Computer Science and Control, Russian Academy of Sciences, Vavilova 40, 119333 Moscow, Russia*

[2]*Institute of Theoretical and Experimental Biophysics, Russian Academy of Sciences, Institutskaya 3, 142290 Pushchino, Moscow Region, Russia*

[3]*Department of Chemistry, Southern Methodist University, Dallas, Texas 75275-0314, USA*

(Received 11 April 2019; published 18 June 2019)

Oscillatory reaction-diffusion fronts are described analytically in a piecewise-linear approximation of the FitzHugh-Nagumo equations with linear cross-diffusion terms, which correspond to a pursuit-evasion situation. Fundamental dynamical regimes of front propagation into a stable and into an unstable state are studied, and the shape of the waves for both regimes is explored in detail. We find that oscillations in the wave profile may either be negligible due to rapid attenuation or noticeable if the damping is slow or vanishes. In the first case, we find fronts that display a monotonic profile of the kink type, whereas in the second case the oscillations give rise to fronts with wavy tails. Further, the oscillations may be damped with exponential decay or undamped so that a saw-shaped pattern forms. Finally, we observe an unexpected feature in the behavior of both types of the oscillatory waves: the coexistence of several fronts with different profile shapes and propagation speeds for the same parameter values of the model, i.e., a multifront regime of wave propagation.

DOI: 10.1103/PhysRevE.99.062214

I. INTRODUCTION

The spatiotemporal behavior of excitable, or active, media exhibits various scenarios of wave and pattern formation, propagation, and interaction. The formalism of reaction-diffusion equations is widely applied to model such phenomena. While the transport in many systems is adequately described by self-diffusion, i.e., the transport of any given species is caused only by its own concentration gradient, there are a considerable number of applications where the transport is affected by the concentration gradients of the other species in the system, giving rise to cross diffusion [1–5]. One of the most well-known reaction-diffusion systems modeling active media is the FitzHugh-Nagumo (FHN) [6,7] equation, also called the Bonhoeffer–van der Pol [8–10] model,

$$\frac{\partial u}{\partial t} = u(1-u)(u-a) - v + D_u\frac{\partial^2 u}{\partial x^2} + h_v\frac{\partial^2 v}{\partial x^2}, \tag{1a}$$

$$\frac{\partial v}{\partial t} = \varepsilon(u-v) + D_v\frac{\partial^2 v}{\partial x^2} + h_u\frac{\partial^2 u}{\partial x^2}, \tag{1b}$$

where the parameters $a, \varepsilon, D_{u,v}$, and $h_{u,v}$ are the excitation threshold, ratio of timescales, and coefficients of self- and cross diffusion, respectively.

Cross-diffusion effects are dominant in systems with strong interactions between particles, for example, long-range electrostatic interactions, in mixtures of aqueous solutions of polymer with micelles (large positive cross-diffusion coefficients), in micelle systems with salt (large negative cross-diffusion coefficients), and in microemulsions due to complexation and excluded volume effects [1]. The FHN model was originally formulated as a simplification of the Hodgkin-Huxley model describing the action potential across a nerve membrane. In this context, the cross-diffusion mechanism reflects the effect of a generic drug on the neuron firing process when the influence of certain drugs or external chemicals alters the normal dynamics of action potential, so that the spatial propagation of neuron firing is essentially caused by the cross diffusion [11]. In an ecological context, the FHN model with cross diffusion describes a pursuit-evasion process in population dynamics with positive taxis of predators up the gradient of prey, pursuit, and negative taxis of prey down the gradient of predators, evasion [12–15].

A new class of nonlinear waves arises in the FHN model with cross diffusion. These waves are also observed in a caricature of the FHN system with a piecewise-linear kinetic function by Rinzel and Keller [16],

$$\frac{\partial u}{\partial t} = -u - v + H(u-a) + h_v\frac{\partial^2 v}{\partial x^2}, \tag{2a}$$

$$\frac{\partial v}{\partial t} = \varepsilon(u-v) - h_u\frac{\partial^2 u}{\partial x^2}, \tag{2b}$$

where $H(u-a)$ is the Heaviside step function. The waves, called "envelope quasisolitons" [15], have some characteristics similar to traveling waves in active media and some similar to solitons. Their morphological features are characterized by oscillatory tails in the spatial profiles. Similar oscillatory behavior may be found in the simple kink-type fronts [17], solitary pulses and wave trains [18], and hybrid pulse-front waves [19]. All those types of waves are the traveling wave solutions of the bistable piecewise-linear FHN model with cross diffusion, whereas the envelope quasisolitons exist in the

*http://www.researchgate.net/profile/Evgeny_Zemskov
†tsyganov@iteb.ru
‡whorsthe@mail.smu.edu

excitable cross-diffusive FHN system [13,15]. The traveling waves display a constant unvarying profile, propagate with constant speed, and can be found analytically for the piecewise linear FHN model [16,20]. The present research focuses on oscillatory traveling waves in the bistable piecewise-linear FHN model related to pursuit-evasion dynamics and pays particular attention to the effects of the cross-diffusion terms. To highlight those effects, we consider the regime where motion due to taxis, i.e., cross diffusion, is dominant. In other words, we neglect self-diffusion and consider the model with pure cross diffusion [13,21,22] in a spatially one-dimensional medium looking for traveling wave solutions of the front type.

Piecewise-linear approximations of the nonlinear kinetic functions represent a widely adopted technique for analytical calculations of the reaction-diffusion equations. Since the pioneering works by McKean [23] and Rinzel and Keller [16], one usually employs a two-piece approximation for the polynomial reaction functions with quadratic and cubic nonlinearities [24–27]. Such approaches reproduce qualitatively the traveling wave dynamics. Highly accurate quantitative results for the wave profile and the propagation speed can be obtained using a piecewise-linear approximation comprising five pieces, as was shown explicitly in the case of cubic and quintic nonlinearities [28]. Clearly, the greater the number of pieces, the more accurate the result of the approximation. In practice, the traveling wave dynamics is reproduced adequately even when only a few segments represent the nonlinear function [28], and we adopt a three-piece approximation for the FHN model, which is sufficient for our purposes [29].

In this study we focus on spatially one-dimensional (1D) systems. In a two-dimensional (2D) medium, wave propagation is more complicated, because of a multiplicity of traveling waves that display different geometries [30,31]. In the regime far from the oscillatory or self-pulsating regime where a Turing-like instability takes place, there exist in the FHN model 2D fronts connecting a stable homogeneous steady state and an extended pattern such as hexagons or quasicrystals [32,33]. However, it is not yet clear how to extend the analytical approach based on the piecewise-linear technique to two-variable 2D reaction-diffusion equations, because it is mathematically difficult to extend the matching conditions from the 1D to the 2D case, fitting the different geometries of the waves.

This paper is organized as follows. In Sec. II we introduce the piecewise-linear FHN model and obtain analytical expressions for the propagating fronts. We apply these results to study the dynamical behavior of fronts propagating into a stable state in Sec. III and into an unstable state in Sec. IV. We discuss our main results in Sec. V.

II. MODEL AND SOLUTIONS

The piecewise-linear FHN model with pure cross-diffusion terms is described by the reaction-diffusion equations

$$\frac{\partial u}{\partial t} = f(u,v) + h\frac{\partial^2 v}{\partial x^2}, \tag{3a}$$

$$\frac{\partial v}{\partial t} = g(u,v) - h\frac{\partial^2 u}{\partial x^2}, \tag{3b}$$

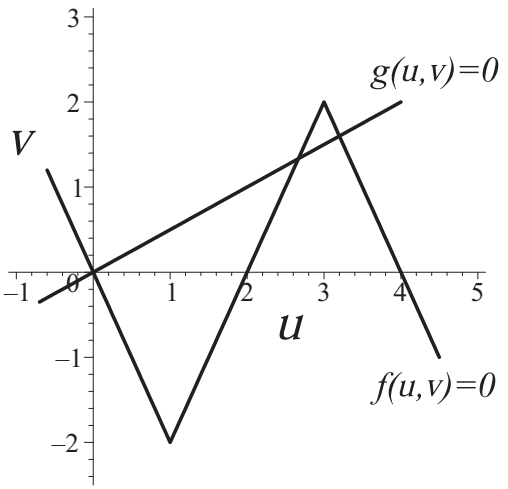

FIG. 1. Nullclines $f(u,v)=0$ and $g(u,v)=0$ for $a=2$ and $b=1/2$.

where the variable $u=u(x,t)$ represents the "activator" or potential variable, the variable $v=v(x,t)$ is the "inhibitor" or recovery variable, and $h_u = h_v \equiv h$ is the cross-diffusion constant. The choice of opposite values for the cross diffusion of the activator and the inhibitor makes our studies specifically relevant to pursuit-evasion situations in predator-prey systems where taxis dominates the motion of individuals. The activator kinetic function $f(u,v)$ consists of three pieces, related to three intervals of u,

$$f(u,v) = \begin{cases} -u - bv, & u \leqslant a/2, \\ u - bv - a, & a/2 < u < 3a/2, \\ -u - bv + 2a, & u \geqslant 3a/2, \end{cases} \tag{4}$$

where b is a positive constant. The inhibitor kinetic function $g(u,v)$ reads

$$g(u,v) = bu - v. \tag{5}$$

The model parameters must be $a>0$ and $0<b<1$ for the system to be bistable. The nullclines $f(u,v)=0$ and $g(u,v)=0$ for the bistable regime are shown in Fig. 1.

The general traveling wave solutions $u=u(\xi)$ and $v=v(\xi)$, where $\xi = x - ct$ is the traveling wave coordinate and c is the propagation speed, satisfy the ordinary differential equations,

$$h\frac{d^2v}{d\xi^2} + c\frac{du}{d\xi} + f(u,v) = 0, \tag{6a}$$

$$-h\frac{d^2u}{d\xi^2} + c\frac{dv}{d\xi} + g(u,v) = 0. \tag{6b}$$

We look for solutions of the form

$$u(\xi) = \sum_n A_n e^{\lambda_n \xi} + u^*, \tag{7a}$$

$$v(\xi) = \sum_n B_n e^{\lambda_n \xi} + v^*, \tag{7b}$$

where A_n, B_n, u^*, and v^* are constants.

Substituting these solutions into (6), we obtain the following matrix equations:

$$\begin{pmatrix} c\lambda - 1 & h\lambda^2 - b \\ -h\lambda^2 + b & c\lambda - 1 \end{pmatrix}\begin{pmatrix} A \\ B \end{pmatrix} = 0 \tag{8}$$

for the first and third intervals and

$$\begin{pmatrix} c\lambda + 1 & h\lambda^2 - b \\ -h\lambda^2 + b & c\lambda - 1 \end{pmatrix}\begin{pmatrix} A \\ B \end{pmatrix} = 0 \tag{9}$$

for the second interval. This yields the characteristic equations

$$(c\lambda - 1)^2 + (h\lambda^2 - b)^2 = 0 \tag{10}$$

for the first and third intervals and

$$(c\lambda)^2 - 1 + (h\lambda^2 - b)^2 = 0 \tag{11}$$

for the second interval. The characteristic equations have the roots

$$\lambda_{1,2} = \frac{1}{2h}[-ic \pm \sqrt{-c^2 + 4h(b + i)}], \tag{12a}$$

$$\lambda_{3,4} = \frac{1}{2h}[ic \pm \sqrt{-c^2 + 4h(b - i)}], \tag{12b}$$

where $i^2 = -1$, for the first and third intervals and

$$\lambda^2_{1-4} = \frac{1}{2h^2}[-(c^2 - 2hb) \pm \sqrt{(c^2 - 2hb)^2 + 4h^2(1 - b^2)}] \tag{13}$$

for the second interval.

Introducing the notations

$$c_b = \frac{c^2}{4h^2} - \frac{b}{h}, \tag{14a}$$

$$y = \sqrt{\frac{1}{2}\left(\sqrt{c_b^2 + 1/h^2} + c_b\right)}, \tag{14b}$$

$$z = \sqrt{\frac{1}{2}\left(\sqrt{c_b^2 + 1/h^2} - c_b\right)}, \tag{14c}$$

we rewrite the roots for the first and third intervals as

$$\lambda_{1,2} = -\frac{ic}{2h} \pm iy \pm z, \tag{15a}$$

$$\lambda_{3,4} = \frac{ic}{2h} \pm iy \mp z. \tag{15b}$$

The final form for the roots for the second interval is

$$\lambda_{1,2} = \pm\frac{1}{\sqrt{2}h}\theta_-, \tag{16}$$

where

$$\theta_- = \sqrt{-(c^2 - 2hb) + \sqrt{(c^2 - 2hb)^2 + 4h^2(1 - b^2)}}, \tag{17}$$

and

$$\lambda_{3,4} = \pm i\frac{1}{\sqrt{2}h}\theta_+, \tag{18}$$

where

$$\theta_+ = \sqrt{c^2 - 2hb + \sqrt{(c^2 - 2hb)^2 + 4h^2(1 - b^2)}}. \tag{19}$$

Consequently, we obtain the general solutions for the first and third intervals as

$$u(\xi) = e^{z\xi}[A_1\cos(p_-\xi) + A_3\sin(p_-\xi)] + e^{-z\xi}[A_2\cos(p_+\xi) + A_4\sin(p_+\xi)] + \hat{u}, \tag{20a}$$

$$v(\xi) = e^{z\xi}[B_1\cos(p_-\xi) + B_3\sin(p_-\xi)] + e^{-z\xi}[B_2\cos(p_+\xi) + B_4\sin(p_+\xi)] + \hat{v}, \tag{20b}$$

where $p_\pm \equiv y \pm c/(2h)$, $(\hat{u}, \hat{v}) = (u^*, v^*)$ for the first interval, and $(\hat{u}, \hat{v}) = (u^{***}, v^{***})$ for the third interval. The general solutions for the second interval are obtained as

$$u(\xi) = A_1e^{\lambda_1\xi} + A_2e^{\lambda_2\xi} + A_3\cos(\theta\xi) + A_4\sin(\theta\xi) + u^{**}, \tag{21a}$$

$$v(\xi) = B_1e^{\lambda_1\xi} + B_2e^{\lambda_2\xi} + B_3\cos(\theta\xi) + B_4\sin(\theta\xi) + v^{**} \tag{21b}$$

with $\theta \equiv \theta_+/(\sqrt{2}h)$. Here the integration constants read

$$B_{1,3} = \frac{(\alpha_-\gamma_- + \beta_-\delta_-)A_{1,3} \pm (\alpha_-\delta_- - \beta_-\gamma_-)A_{3,1}}{\gamma_-^2 + \delta_-^2}, \tag{22a}$$

$$B_{2,4} = \frac{(\alpha_+\gamma_+ - \beta_+\delta_+)A_{2,4} \pm (\alpha_+\delta_+ + \beta_+\gamma_+)A_{4,2}}{\gamma_+^2 + \delta_+^2}, \tag{22b}$$

where

$$\alpha_\pm = b - h(z^2 - p_\pm^2), \quad \beta_\pm = 2hzp_\pm, \tag{23a}$$

$$\gamma_\pm = 1 \pm cz, \quad \delta_\pm = cp_\pm \tag{23b}$$

for the first and third intervals and

$$B_{1,2} = \frac{1}{1 - c\lambda_{1,2}}\left(b - h\lambda_{1,2}^2\right)A_{1,2}, \tag{24a}$$

$$B_{3,4} = \frac{1}{1 + c^2\theta^2}(b + h\theta^2)(A_{3,4} \pm c\theta A_{4,3}) \tag{24b}$$

for the second interval.

We now construct particular solutions for the basic type of waves, traveling fronts, using these general solutions. The particular solutions are built from different parts that correspond to the various intervals.

III. PROPAGATION INTO A STABLE STATE

The simplest particular solution is a standard front of the kink type. Such a front connects the intersection points in the first and third pieces of the nullclines, i.e., the fixed points, and consists of three parts, $u_{1,2,3}$ and $v_{1,2,3}$, for the activator and inhibitor variable, respectively. We will call these waves 3-fronts for the sake of brevity. The boundary conditions for the front solutions are as follows: $(u_1, v_1)(\xi \to -\infty) = (0, 0)$ for the first fixed point and $u_3(\xi \to +\infty) = 2a/(1 + b^2)$ and $v_3(\xi \to +\infty) = 2ab/(1 + b^2)$ for the second fixed point, so

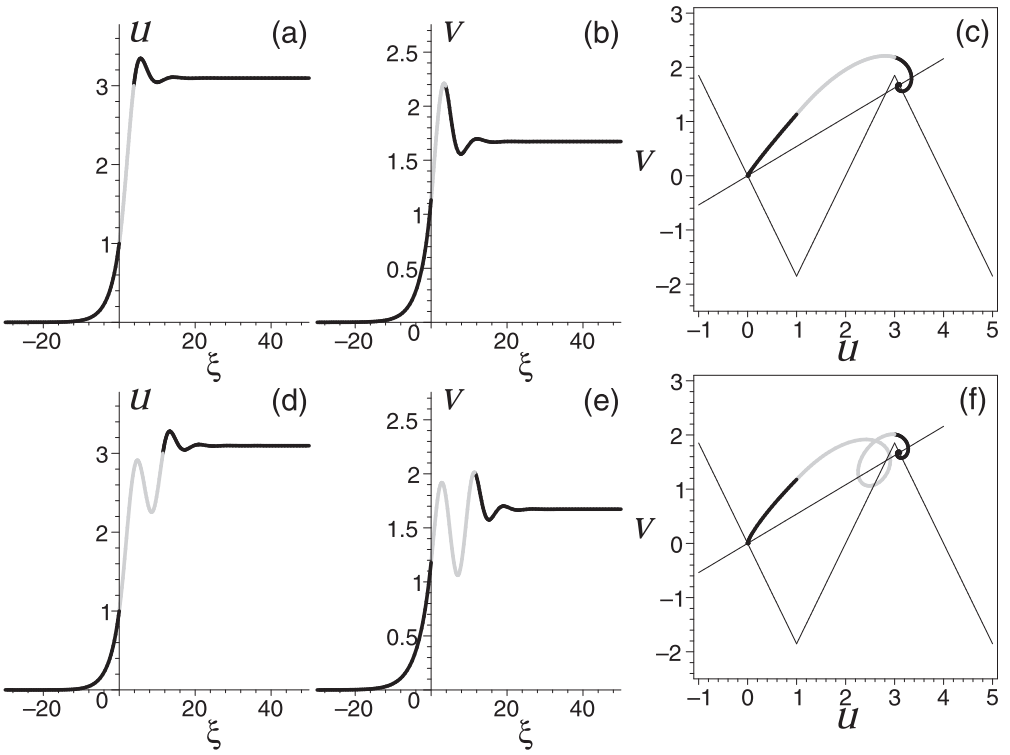

FIG. 2. Front profiles for the activator $u(\xi)$ (a), (d), for the inhibitor $v(\xi)$ (b), (e), and in the u-v phase plane (bold lines) (c), (f). The parameter values are fixed at $a = 2$, $b = 0.54$, and $h = 4$. The middle parts, u_2 and v_2, of the fronts are indicated by gray. The nullclines $f(u, v) = 0$ and $g(u, v) = 0$ are shown by thin lines in panels (c), (f). The calculated propagation speed is $c \approx 2.949$ (a)–(c) and $c \approx 3.407$ (d)–(f).

that the front solutions read

$$u_1(\xi) = e^{z\xi}[A_{11}\cos(p_-\xi) + A_{13}\sin(p_-\xi)], \tag{25a}$$

$$u_2(\xi) = A_{21}e^{\lambda_1\xi} + A_{22}e^{\lambda_2\xi} + A_{23}\cos(\theta\xi) + A_{24}\sin(\theta\xi) + a/(1-b^2), \tag{25b}$$

$$u_3(\xi) = e^{-z\xi}[A_{32}\cos(p_+\xi) + A_{34}\sin(p_+\xi)] + 2a/(1+b^2) \tag{25c}$$

for the activator variable and

$$v_1(\xi) = e^{z\xi}[B_{11}\cos(p_-\xi) + B_{13}\sin(p_-\xi)], \tag{26a}$$

$$v_2(\xi) = B_{21}e^{\lambda_1\xi} + B_{22}e^{\lambda_2\xi} + B_{23}\cos(\theta\xi) + B_{24}\sin(\theta\xi) + ab/(1-b^2), \tag{26b}$$

$$v_3(\xi) = e^{-z\xi}[B_{32}\cos(p_+\xi) + B_{34}\sin(p_+\xi)] + 2ab/(1+b^2) \tag{26c}$$

for the inhibitor variable. These three parts of the front solutions are joined together using the matching conditions for the pieces $u_n(\xi)$, $v_n(\xi)$, $n = 1, \ldots, 3$, and their derivatives $du_n(\xi)/d\xi$, $dv_n(\xi)/d\xi$, at the two matching points, $\xi = \xi_0$ and $\xi = \xi_0^*$:

$$u_1(\xi_0) = u_2(\xi_0), \quad \frac{du_1(\xi_0)}{d\xi} = \frac{du_2(\xi_0)}{d\xi}, \tag{27a}$$

$$u_2(\xi_0^*) = u_3(\xi_0^*), \quad \frac{du_2(\xi_0^*)}{d\xi} = \frac{du_3(\xi_0^*)}{d\xi}, \tag{27b}$$

$$v_1(\xi_0) = v_2(\xi_0), \quad \frac{dv_1(\xi_0)}{d\xi} = \frac{dv_2(\xi_0)}{d\xi}, \tag{27c}$$

$$v_2(\xi_0^*) = v_3(\xi_0^*), \quad \frac{dv_2(\xi_0^*)}{d\xi} = \frac{dv_3(\xi_0^*)}{d\xi}. \tag{27d}$$

The values of $u(\xi)$ at the matching points ξ_0 and ξ_0^* are known, which yields two additional equations,

$$u_1(\xi_0) = a/2, \quad u_3(\xi_0^*) = 3a/2. \tag{28}$$

In total, there are 10 equations for 10 unknown constants (eight integration constants A, second matching point coordinate, and the front speed c), which allow us to determine the front speed and the second matching point uniquely. The first matching point is chosen to be zero due to the translational invariance of the equations.

The profiles of the front waves are shown for positive values of the cross-diffusion coefficient h in Fig. 2 and for negative values in Fig. 3. The corresponding speed diagrams are displayed in Figs. 4(a) and 4(b), respectively. The figures for the front profiles show that for a given value of h there exist several fronts that differ in profile shape and speed value. For positive h (Fig. 2), we found two 3-fronts, the fast and slow waves. The slow wave is monotonic in the middle part of the wave profile [Figs. 2(a)–2(c)], whereas the fast wave has a zigzag in the middle part [Figs. 2(d) and 2(e)] that corresponds to a loop in the (u, v)-phase plane [Fig. 2(f)]. The decaying edge parts exhibit oscillations on the right side, the third part,

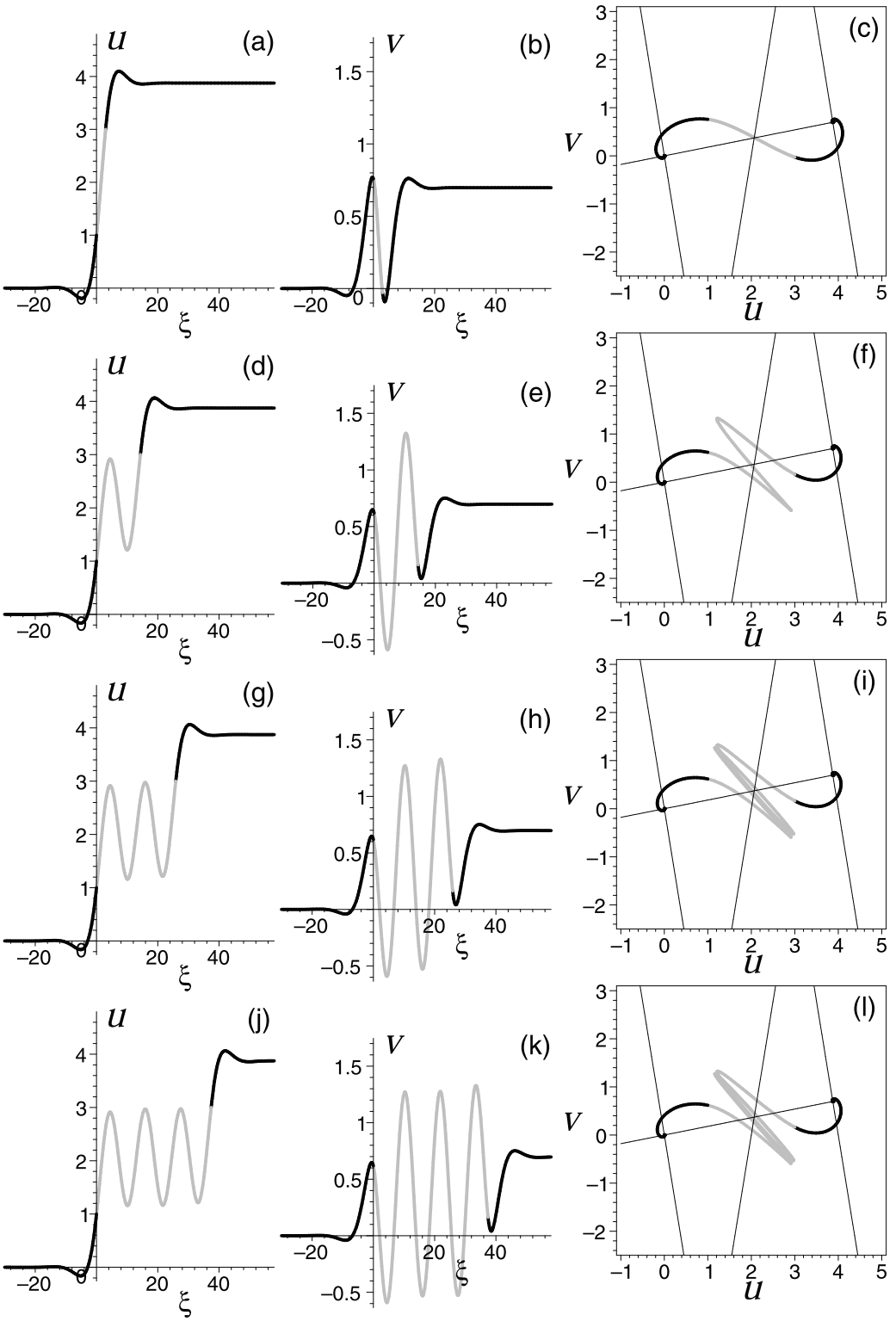

FIG. 3. Front profiles for the activator $u(\xi)$ (a), (d), (g), (j), for the inhibitor $v(\xi)$ (b), (e), (h), (k), and in the u-v phase plane (bold lines) (c), (f), (i), (l). The parameter values are fixed at $a = 2$, $b = 0.18$, and $h = -4$. The middle parts, u_2 and v_2, of the fronts are indicated by gray. The nullclines $f(u, v) = 0$ and $g(u, v) = 0$ are shown by thin lines in panels (c), (f), (i), (l). The calculated propagation speed is $c \approx -0.14$ (a)–(c), $c \approx -0.160178$ (d)–(f), $c \approx -0.160299$ (g)–(i), and $c \approx -0.160300$ (j)–(l).

for waves, so that they form a spiral in the phase plane. In fact, one can find also front waves with many zigzags or loops for the same values of the model parameters. However, such waves are outside the scope of our study here, because the second and next zigzags or loops intersect the boundary between the second and third interval, i.e., they do not fit the three-piece construction of fronts described here. Thus, the speed diagram [Fig. 4(a)] shows only the two waves discussed

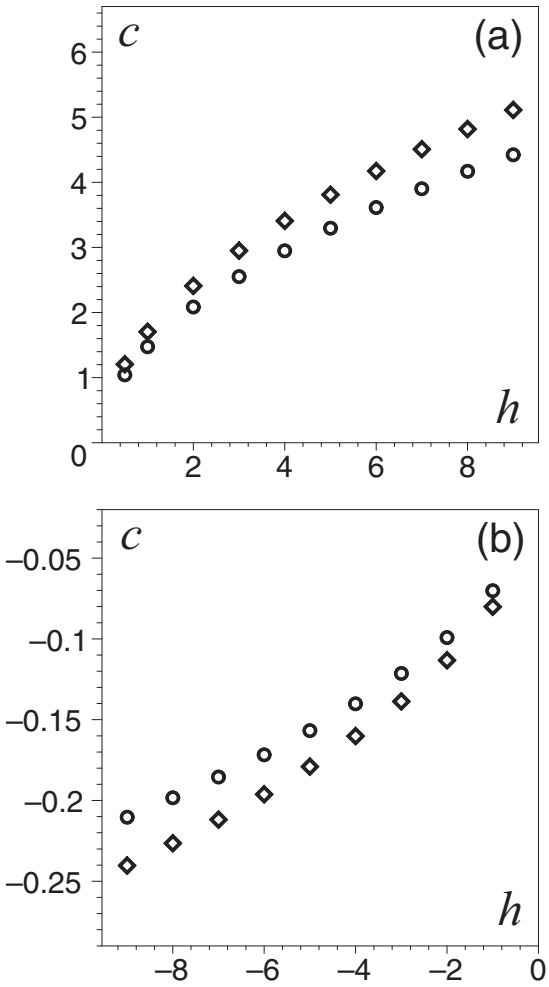

FIG. 4. Speed of the front as a function of the cross-diffusion coefficient, $c = c(h)$, for (a) positive and (b) negative values of h. The fronts with monotonic and nonmonotonic (zigzags) middle part are marked by circles and diamonds, respectively. The model parameters are fixed at $a = 2$, (a) $b = 0.54$, and (b) $b = 0.18$.

above. The speed values of both fronts increase when the cross-diffusion coefficient is increased.

The situation as regards the number of 3-fronts changes significantly for negative h (Fig. 3). In this case, together with the slow wave with a monotonic middle part profile [Figs. 3(a)–3(c)], there exist several fast waves with pronounced oscillations located in the middle part of the wave profile, so that the 3-fronts can have one [Figs. 3(d)–3(f)], two [Figs. 3(g)–3(i)], three [Figs. 3(j)–3(l)], and more zigzags. We have determined and presented here only the first three waves with zigzags in the middle part of the wave profile, but we expect that waves with a greater number zigzags exist. The limiting case when the number of zigzags goes to infinity corresponds to the two-piece front that is located in the first and the second intervals. This evolution of the oscillations in the middle part of the wave profile motivated our investigation of traveling fronts related to the first and second pieces of the nullclines, i.e., the propagation into an unstable state; see the next section.

The speed values of the fast waves for negative h do not differ much from each other for a fixed value of h. Also, as the number of zigzags increases, the difference in speed values decreases. This feature is reflected in the speed diagram [Fig. 4(b)]. There appear again only two visually distinct branches of points that correspond to the two types of waves, the slow (with a monotonic middle part of the wave profile) and the fast (with oscillations in the middle part) fronts. All fast fronts have almost the same speed values and show as only one branch on the speed diagram.

IV. PROPAGATION INTO AN UNSTABLE STATE

The fronts discussed in the previous section propagate from one stable state into another. However, in the model we study, there exist also fronts that can propagate into an unstable state related to the fixed point in the second interval; i.e., these fronts connect intersection points in the first and second pieces of nullclines and therefore consist of two parts, $u_{1,2}$ and $v_{1,2}$, for the activator and inhibitor variables, respectively. We will call these waves 2-fronts for the sake of brevity. Since in the second interval $\lambda_1 > 0, \lambda_2 < 0$ for $h > 0$ and $\lambda_1 < 0, \lambda_2 > 0$ for $h < 0$ [see Eq. (16)], the boundary conditions require $A_{21} = 0$ and $B_{21} = 0$ for $h > 0$ and $A_{22} = 0$ and $B_{22} = 0$ for $h < 0$, so that the front solutions read for $h > 0$,

$$u_1(\xi) = e^{z\xi}[A_{11}\cos(p_-\xi) + A_{13}\sin(p_-\xi)], \tag{29a}$$

$$u_2(\xi) = A_{22}e^{\lambda_2\xi} + A_{23}\cos(\theta\xi) + A_{24}\sin(\theta\xi) + a/(1-b^2) \tag{29b}$$

for the activator variable and

$$v_1(\xi) = e^{z\xi}[B_{11}\cos(p_-\xi) + B_{13}\sin(p_-\xi)], \tag{30a}$$

$$v_2(\xi) = B_{22}e^{\lambda_2\xi} + B_{23}\cos(\theta\xi) + B_{24}\sin(\theta\xi) + ab/(1-b^2) \tag{30b}$$

for the inhibitor variable. For $h < 0$, we find

$$u_1(\xi) = e^{z\xi}[A_{11}\cos(p_-\xi) + A_{13}\sin(p_-\xi)], \tag{31a}$$

$$u_2(\xi) = A_{21}e^{\lambda_1\xi} + A_{23}\cos(\theta\xi) + A_{24}\sin(\theta\xi) + a/(1-b^2) \tag{31b}$$

for the activator variable and

$$v_1(\xi) = e^{z\xi}[B_{11}\cos(p_-\xi) + B_{13}\sin(p_-\xi)], \tag{32a}$$

$$v_2(\xi) = B_{21}e^{\lambda_1\xi} + B_{23}\cos(\theta\xi) + B_{24}\sin(\theta\xi) + ab/(1-b^2) \tag{32b}$$

for the inhibitor variable. Now there are one matching point and five matching equations for five unknown integration constants A. In contrast to the case of the propagation into a stable state, the boundary conditions for this case do not specify a unique solution. In fact, there exists a family of solutions that correspond to waves propagating at different speeds. The front speed c is not calculated from the matching equations but is chosen *a priori*. The only restriction remains the same

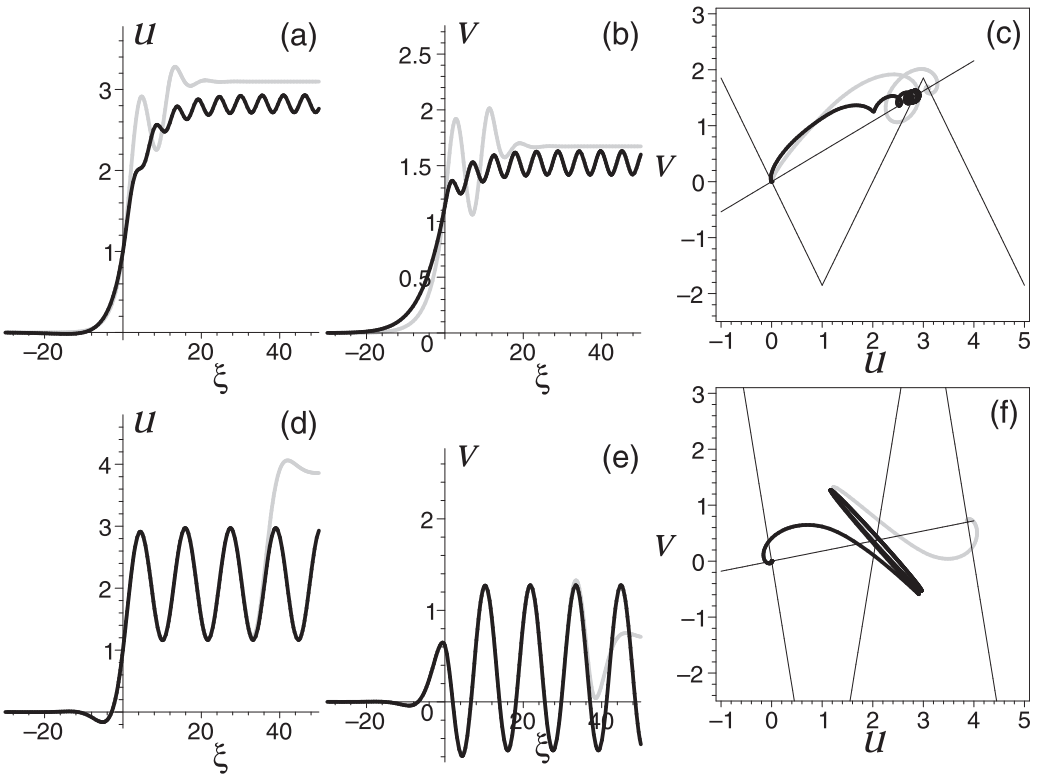

FIG. 5. Comparison of front propagation into an unstable (black) and a stable (gray) state. Wave profiles are shown for the activator $u(\xi)$ (a), (d), for the inhibitor $v(\xi)$ (b), (e), and in the u-v phase plane (bold lines) (c), (f). The parameter values are fixed at $a = 2$, (a)–(c) $b = 0.54$, $h = 4$, and (d)–(f) $b = 0.18$, $h = -4$. The calculated speed of the front propagating into a stable state is (a)–(c) $c \approx 3.407$ and (d)–(f) $c \approx -0.1603$. The speed of the front propagating into an unstable state is chosen as (a)–(c) $c = 5$ and (d)–(f) $c = -0.16$. The nullclines $f(u, v) = 0$ and $g(u, v) = 0$ are shown by thin lines in panels (c), (f).

as above; the waves must be inside the scope of our study. In other words, they do not intersect the boundary between the second and third intervals, because they are related to the two-piece construction of fronts described above. Therefore, a comparison of the 2- and 3-fronts for the same value of the propagation speed is impossible for positive h. For $h < 0$, both fronts with the same speed value can be compared; see Fig. 5. This comparison shows that the 3-front approaches the 2-front when the number of zigzags in the second part tends to infinity. The correspondence of the two types of waves is already quite close for three zigzags, as illustrated graphically in Figs. 5(d)–5(f).

An infinite number of zigzags gives rise to a saw-shaped pattern that manifests undamped oscillations in the wave profile. Such fronts, called wavy wave fronts, have been described by Carpio and Bonilla [34] in a chain of nonlinear oscillators that are diffusively coupled and subject to an external constant force. In fact, it represents a spatially discrete version of a hyperbolic reaction-diffusion system, where traveling fronts with exponentially decaying oscillatory tails have been found [27,35,36]. The undamped oscillations in the front profile can be obtained by a periodic traveling-wave modulation, a periodic comoving forcing, in the bistable reaction-diffusion equation [37]. Similar modulated wave fronts propagating into an unstable state have been reported for a modified Swift-Hohenberg equation describing an optical system [38].

V. CONCLUSIONS

We have studied the effects of cross diffusion on the nonlinear wave dynamics of the FitzHugh-Nagumo reaction-diffusion system. To focus attention on the impact of cross diffusion, we have considered the case where the self-diffusion coefficients vanish. The cross-diffusion coefficient is chosen to have opposite values for the activator and for inhibitor, corresponding to a pursuit-evasion situation in a population dynamics context. We have adopted the McKean-type piecewise-linear version of the kinetic term in the activator equation to be able to obtain analytical results. Specifically, we have used a kinetic term consisting of three pieces.

The regimes of fronts propagating into a stable state as well as into an unstable state were studied. Analytical expressions for the traveling fronts were obtained in both cases. The profile of the fronts can be monotonic of the kink type or display a succession of oscillations. Our second main result is the finding that a multifront regime of wave propagation occurs in the system, i.e., the coexistence of several fronts with different profile shapes and different values of propagation speed for the same parameter values of the model. Our results are a further illustration of the rich dynamical behavior of the FitzHugh-Nagumo model with cross diffusion.

We suggest two directions in which these studies could be extended. First, piecewise-linear models are a widely adopted and accepted technique to study the dynamical behavior of

nonlinear reaction-diffusion equations, since they possess the significant advantage of allowing us to obtain analytical results. It is, however, certainly worthwhile to study the original fully nonlinear FHN model to confirm our expectation that the various wave regimes described here also occur in that model as long-time asymptotic solutions. Second, it is well known that propagating fronts in reaction-diffusion systems can be affected by noise; see, for example, Refs. [39–41]. The specific effects of the noise will depend on its specific nature: internal fluctuations or external noise, white noise or correlated noise, etc. We expect that the fronts described in Sec. III, propagating into a stable state, will be fairly robust against noise, at least in the weak noise regime, and the effects will be subtle [41]. On the other hand, fluctuations could strongly affect the fronts described in Sec. IV, propagating into an unstable state, [39,40] and could alter their dynamics significantly, such as the oscillations in the wave profile.

[1] V. K. Vanag and I. R. Epstein, Cross-diffusion and pattern formation in reaction–diffusion systems, Phys. Chem. Chem. Phys. **11**, 897 (2009).

[2] A. Madzvamuse and R. Barreira, Exhibiting cross-diffusion-induced patterns for reaction-diffusion systems on evolving domains and surfaces, Phys. Rev. E **90**, 043307 (2014).

[3] M. A. Budroni, Cross-diffusion-driven hydrodynamic instabilities in a double-layer system: General classification and nonlinear simulations, Phys. Rev. E **92**, 063007 (2015).

[4] G. Gambino, M. C. Lombardo, and M. Sammartino, Turing instability and traveling fronts for a nonlinear reaction–diffusion system with cross-diffusion, Math. Comp. Simul. **82**, 1112 (2012).

[5] G. Gambino, M. C. Lombardo, and M. Sammartino, Cross-diffusion-induced subharmonic spatial resonances in a predator-prey system, Phys. Rev. E **97**, 012220 (2018).

[6] R. FitzHugh, Impulses and physiological states in theoretical models of nerve membrane, Biophys. J. **1**, 445 (1961).

[7] J. Nagumo, S. Arimoto, and S. Yoshizawa, An active pulse transmission line simulating nerve axon, Proc. IRE **50**, 2061 (1962).

[8] B. van der Pol, On relaxation-oscillations, Phil. Mag. **2**, 978 (1926).

[9] K. F. Bonhoeffer, Über die Aktivierung von passivem Eisen in Salpetersäure, Z. Elektrochem. **47**, 147 (1941).

[10] K. F. Bonhoeffer, Activation of passive iron as a model for the excitation of nerve, J. Gen. Physiol. **32**, 69 (1948).

[11] F. Berezovskaya, E. Camacho, S. Wirkus, and G. Karev, "Traveling wave" solutions of FitzHugh model with cross-diffusion, Math. Biosci. Eng. **5**, 239 (2008).

[12] M. A. Tsyganov, J. Brindley, A. V. Holden, and V. N. Biktashev, Quasisoliton Interaction of Pursuit-Evasion Waves in a Predator-Prey System, Phys. Rev. Lett. **91**, 218102 (2003).

[13] V. N. Biktashev and M. A. Tsyganov, Solitary waves in excitable systems with cross-diffusion, Proc. Royal Soc. A **461**, 3711 (2005).

[14] M. A. Tsyganov, V. N. Biktashev, J. Brindley, A. V. Holden, and G. R. Ivanitskii, Waves in systems with cross-diffusion as a new class of nonlinear waves, Phys. Uspekhi **50**, 263 (2007).

[15] V. N. Biktashev and M. A. Tsyganov, Envelope Quasisolitons in Dissipative Systems with Cross-Diffusion, Phys. Rev. Lett. **107**, 134101 (2011).

[16] J. Rinzel and J. B. Keller, Traveling wave solutions of a nerve conduction equation, Biophys. J. **13**, 1313 (1973).

[17] E. P. Zemskov, K. Kassner, and M. J. B. Hauser, Wavy fronts and speed bifurcation in excitable systems with cross diffusion, Phys. Rev. E **77**, 036219 (2008).

[18] E. P. Zemskov, M. A. Tsyganov, and W. Horsthemke, Oscillatory pulses and wave trains in a bistable reaction-diffusion system with cross diffusion, Phys. Rev. E **95**, 012203 (2017).

[19] E. P. Zemskov, M. A. Tsyganov, and W. Horsthemke, Oscillatory pulse-front waves in a reaction-diffusion system with cross diffusion, Phys. Rev. E **97**, 062206 (2018).

[20] J. Rinzel and D. Terman, Propagation phenomena in a bistable reaction-diffusion system, SIAM J. Appl. Math. **42**, 1111 (1982).

[21] E. P. Zemskov and A. Yu. Loskutov, Oscillatory traveling waves in excitable media, J. Exper. Theor. Phys. **107**, 344 (2008).

[22] E. P. Zemskov, I. R. Epstein, and A. Muntean, Oscillatory pulses in FitzHugh–Nagumo type systems with cross-diffusion, Math. Med. Biol. **28**, 217 (2011).

[23] H. P. McKean, Nagumo's equation, Adv. Math. **4**, 209 (1970).

[24] A. Ito and T. Ohta, Self-organization in an excitable reaction-diffusion system. III. Motionless localized versus propagating-pulse solutions, Phys. Rev. A **45**, 8374 (1992).

[25] V. Méndez and J. Camacho, Dynamics and thermodynamics of delayed population growth, Phys. Rev. E **55**, 6476 (1997).

[26] V. Méndez and J. E. Llebot, Hyperbolic reaction-diffusion equations for a forest fire model, Phys. Rev. E **56**, 6557 (1997).

[27] G. Abramson, A. R. Bishop, and V. M. Kenkre, Effects of transport memory and nonlinear damping in a generalized Fisher's equation, Phys. Rev. E **64**, 066615 (2001).

[28] S. Theodorakis and E. Svoukis, Piecewise linear emulation of propagating fronts as a method for determining their speeds, Phys. Rev. E **68**, 027201 (2003).

[29] R. Bakanas, Travelling fronts in a piecewise-linear bistable system, Nonlinearity **16**, 313 (2003).

[30] P. K. Brazhnik and J. J. Tyson, Travelling waves and static structures in a two-dimensional exactly solvable reaction-diffusion system, J. Phys. A **32**, 8033 (1999).

[31] P. K. Brazhnik and J. J. Tyson, On traveling wave solutions of Fisher's equation in two spatial dimensions, SIAM J. Appl. Math. **60**, 371 (1999).

[32] M. Bachir, P. Borckmans, and G. Dewel, Spatial multistability and nonvariational effects, Phys. Rev. E **59**, R6223(R) (1999).

[33] M. Tlidi, G. Sonnino, and M. Bachir, Predicted formation of localized superlattices in spatially distributed reaction-diffusion solutions, Phys. Rev. E **86**, 045103(R) (2012).

[34] A. Carpio and L. L. Bonilla, Oscillatory wave fronts in chains of coupled nonlinear oscillators, Phys. Rev. E **67**, 056621 (2003).

[35] K. K. Manne, A. J. Hurd, and V. M. Kenkre, Nonlinear waves in reaction-diffusion systems: The effect of transport memory, Phys. Rev. E **61**, 4177 (2000).

[36] E. P. Zemskov, M. A. Tsyganov, and W. Horsthemke, Wavy fronts in a hyperbolic FitzHugh-Nagumo system and the effects of cross diffusion, Phys. Rev. E **91**, 062917 (2015).

[37] E. P. Zemskov, K. Kassner, and S. C. Müller, Front propagation under periodic forcing in reaction-diffusion systems, Eur. Phys. J. B **34**, 285 (2003).

[38] C. Durniak, M. Taki, M. Tlidi, P. L. Ramazza, U. Bortolozzo, and G. Kozyreff, Modulated optical structures over a modulationally stable medium, Phys. Rev. E **72**, 026607 (2005).

[39] J. García-Ojalvo and J. M. Sancho, *Noise in Spatially Extended Systems* (Springer-Verlag, New York, 1999).

[40] D. Panja, Effects of fluctuations on propagating fronts, Phys. Rep. **393**, 87 (2004).

[41] E. Khain, Y. T. Lin, and L. M. Sander, Fluctuations and stability in front propagation, Europhys. Lett. **93**, 28001 (2011).